Eldad Bahat-Treidel (Autor)

GaN-Based HEMTs for High Voltage Operation: Design, Technology and Characterization

https://cuvillier.de/de/shop/publications/6087

Copyright:
Cuvillier Verlag, Inhaberin Annette Jentzsch-Cuvillier, Nonnenstieg 8, 37075 Göttingen, Germany
Telefon: +49 (0)551 54724-0, E-Mail: info@cuvillier.de, Website: https://cuvillier.de

Chapter 1

Introduction

Unintentional coincidence had led to intercept the GaN-power electronics' destiny with my own. As a lithography process engineer in the Si industry I expended my horizons towards optoelectronic engineering. Thus, my initial intention in the Ferdinand-Braun-Institut, Leibniz-Institut für Höchstfrequenztechnik (FBH) was to conduct my PhD work in the optoelectronic department. This trivial course was interrupted as I was assigned to the GaN electronics business area to develop high breakdown voltage capabilities of GaN-based HEMTs for switching applications in satellites. The GaN electronics business area group in the FBH was assigned to carry out the Radiation-Hardness GaN-based HEMT for space applications project. The goal of this project is the development of GaN-based radiation hardened with high breakdown voltage switching transistors and regulators as an alternative to Si-based power MOSFETs for Electric Power Conditioner (EPC) in the next generation of Travelling Wave Tube Amplifiers (TWTA) in satellites.

GaN-based semiconductor electronics was foreign to me as the surface of the moon, but I was immediately charmed with its properties and merits. Although I must admit that in the beginning transistors with neither native oxide and polysilicon gates, nor *p*-*n* junctions and implanted ohmic contacts were miraculous to me. But most amazing for me was the existence of two-dimensional-electron-gas (2DEG) channel under the thin AlGaN barrier that is created by polarization differences between the two wide-bandgap materials. Throughout this time I recognized and prevailed enormous challenges in the GaN-based HEMTs through device simulations, device design, processing and characterization.

Dieses Werk ist copyrightgeschützt und darf in keiner Form vervielfältigt werden noch an Dritte weitergegeben werden.
Es gilt nur für den persönlichen Gebrauch.

1.1. Radiation Hardness GaN-Based HEMTs' Project Specifications

GaN-based semiconductor holds particular promise for the space sector. It can reliably operate at much higher voltages and temperatures than widely-used semiconductors such as silicon (Si) or gallium arsenide (GaAs), and is also inherently radiation-hard [1]. When used to realize space-based microwave and power devices, GaN should enable reduction in the size and mass of cooling systems, an enhanced ability to survive the hard radiation environment of deep space with superior output power [2].One of the most attractive concepts is replacement high voltage power Si MOSFETs with GaN-based HEMTs in the satellite communications power systems. Key components for communications satellites are the power amplifiers in the telecommunications payload. Travelling Wave Tube Amplifier (TWTA) is a key element for a satellite transponder. The TWTA consists of the Travelling Wave Tube (TWT) mainly determining the RF performance and the Electronic Power Conditioner (EPC), designed and manufactured for power matching of the DC and bus interfaces.

The developed devices intended to replace existing Si based MOSFET power devices. Therefore they obliged to be compatible with their electrical specifications. Examples for commercial devices with comparable specifications are IRHNA57264SE for switching applications and IRHY7G30CMSE for regulation applications [3]. The radiation hardness GaN-Based HEMTs project explicitly defined the following specifications for the developed devices:

Tolerance to ionizing radiation, TID (gamma)	100-300 krad (Si)
Single Event Effect, (SEE), (heavy ion) with linear energy transfer, (LET):	14-82 MeV/(mg/cm^2), 150-460 MeV
Lifetime:	> 20 years
Devices for switching application:	250 V normally-off very low R_{ON} of 50 mΩ I_D of 150 A
Devices for regulation application:	1000 V normally-on and normally-off R_{ON} of 5000 mΩ I_D of 5 A
Flip chip assembly	

Table 1.1–1 General specifications for radiation hardness AlGaN/GaN HEMTs.

In the radiation hardness GaN-based HEMTs development project's work frame four major phases were defined:

Phase 1: Concepts and feasibility studies for breakdown voltage and for radiation hardness on test structures. Develop reliable of flip-chip technology.

Phase 2: Development of normally-on devices with $V_{BR\ OFF} > 550$ V and normally-off devices $V_{BR\ OFF} > 250$ V for switching application.

Phase 3: Development of normally-on and normally-off devices with $V_{BR\ OFF} > 1000$ V for regulation application.

Phase 4: Radiation hardness and reliability tests.

Dieses Werk ist copyrightgeschützt und darf in keiner Form vervielfältigt werden noch an Dritte weitergegeben werden.
Es gilt nur für den persönlichen Gebrauch.

1.2. Problem Definition, Scope of Work and Success Criteria

Prior to this project, GaN-Based HEMT's in FBH were designed as microwave power amplifiers for high frequency operation with high output power and high power added efficiency. Such design focused on high current, high gain, low RF losses and low RF dispersion. In such design the OFF-state breakdown voltage has less importance. On the other hand the microwave design and process was a fertile ground for high voltage power switching devices due to its basic merits such as high carrier density, very low ohmic contact resistance and ON-state resistance. Therefore the task was to design GaN-based switching devices with enhanced OFF-state blocking capability while preserving as much as possible other device electrical properties.

The power devices' chart depicts, in Figure 1.2–1, the GaN, Si and SiC-based state-of-the-art power devices vs. typical microwave design test devices, $1\ \mu m \geq L_{GD} \geq 10\ \mu m$, from FBH at the starting point of this work. It could be seen that such devices have much lower ON-state resistance than the compared devices but suffers from lack of OFF-state blocking capability. At that time such devices were far from the GaN material limitation using its superior breakdown field.

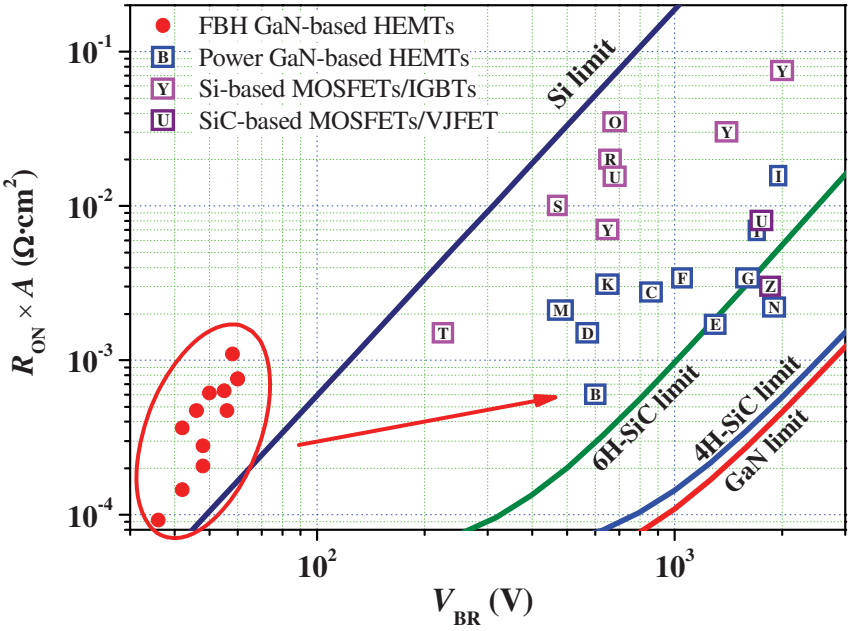

Figure 1.2–1 OFF-state breakdown voltage, $V_{BR\ OFF}$, vs. $R_{ON} \times A$ of the fabricated GaN-based HEMTs from FBH at the project starting point compared with those of the state-of-the-art Si, SiC and GaN-based devices. The theoretical limitations of different device families are taken from literature see section 2.4.2.

Dieses Werk ist copyrightgeschützt und darf in keiner Form vervielfältigt werden noch an Dritte weitergegeben werden.
Es gilt nur für den persönlichen Gebrauch.

Points	Year	Group	Technology	$R_{ON} \times A$ ($\Omega \cdot cm^2$)	$V_{BR\ OFF}$ (V)
B	2005	Saito *et al.* [4]	GaN HEMT	0.0006	600
C	2004	Huili *et al.* [5]	GaN HEMT	0.0028	860
D	2000	Zhang *et al.* [6]	GaN HEMT	0.0015	570
E	2002	Zhang *et al.* [7]	GaN HEMT	0.0017	1300
F	2001	Zhang *et al.* [8]	GaN HEMT	0.0034	1050
G	2006	Tipirneni *et al.* [9]	GaN HEMT	0.0034	1600
I	2006	Yagi *et al.* [10]	GaN HEMT	0.0069	1700
K	2007	Morita *et al.* [11]	GaN HEMT	0.0031	650
M	2007	Saito *et al.* [12]	GaN HEMT	0.0021	480
N	2006	Dora *et al.* [13]	GaN HEMT	0.0022	1900
O	2000	Infineon CoolMOS™ [14]	Si MOSFET	0.035	680
R	2006	Fuji SJ-MOSFET [15]	Si MOSFET	0.02	658
S	2005	Philips RESERF MOSFET [16]	Si MOSFET	0.0098	473
T	2006	Denso/Toyota SJ-MOSFET [17]	Si MOSFET	0.0015	225
Y	Range	Range	Si IGBT	Range	Range
U	2008	Cree MOSFET [18]	SiC MOSFET	0.008	1750
Z	2008	Semisouth VJFET [18]	SiC VJFET	0.003	1850

Table 1.2–1 OFF-state breakdown voltage, $V_{BR\ OFF}$ vs. $R_{ON} \times A$ data.

1.2.1. Scope and Schedule of This Work

The scope of this work is a derivative of the complete radiation hardness GaN-based switching transistors project. In this part of the project, enhancement of the OFF-state blocking voltage to 1000 V while keeping the ON-state resistance as low as possible is desired. The development in this work should have followed the milestones in the project and therefore it was divided to 4 predefined working stages:

Stage 1: Seeking for concepts and feasibility studies for breakdown voltage using physically based simulation and electrical measurements analysis.

Stage 2: Develop normally-on devices with OFF-state blocking capability of $V_{BR\ OFF} > 550$ V and $V_{BR\ OFF} > 250$ V to create the foundations switching application.

Stage 3: Develop normally-on devices with OFF-state blocking capability $V_{BR\ OFF} > 1000$ V to create the foundations to regulation application.

Stage 4: Transfer the developed technology to power device with high voltage and large area.

Schedule	2006		2007				2008				2009			
	Q3	Q4	Q1	Q2	Q3	Q4	Q1	Q2	Q3	Q4	Q1	Q2	Q3	Q4
Simulations of the device electrical properties and device characterization matching.					← Ongoing →									
Identification of tools and methods to enhance the device breakdown voltage							← Ongoing →							
Experimental verification of the device design performance and iterations.														
Transfer to power device with high voltage and scale-up.														

Table 1.2–2 This work principal schedule and milestones' Gantt-chart.

Principal schedule Gantt-chart for this work is shown in Table 1.2–2. Follow the development of the simulation tools for device design characterization and analysis it is desired to use it as an ongoing engineering tool in a feedback loop from the experimental results. The development of tools and methods for breakdown voltage enhancement in the

Dieses Werk ist copyrightgeschützt und darf in keiner Form vervielfältigt werden noch an Dritte weitergegeben werden.
Es gilt nur für den persönlichen Gebrauch.

device is also an ongoing task along the experimental verification of the proposed devices, as described along this work.

Tasks in this work should be solved by the following means; Simulation and design of epitaxial layers structures optimized to extract the merits of the GaN material system. Design device geometry (field plates, layout etc.) to reduce critical electric fields and reduce the subthreshold leakages in the device. Process modifications and adjustments that may have influence on the high voltage characteristics of the devices should be considered. Last but not list, are the electrical measurements and analysis of the devices at high voltage.

In addition support to other projects such as the S-class switching amplifier was given. Here it was desired integrate a reverse high voltage bias protection diode into the GaN-based HEMT. Such diode should protect the microwave power HEMT that may experience a short negative pulse at the drain terminal as a result of a fly-back signal from the output filter.

1.2.2. The Flow of This Work

Chapter 2 covers the essential background on GaN-based HEMTs required for this work. GaN-based semiconductor material properties and merits are reviewed. GaN-based HEMT device principal operation is enlightened. Brief description of the device manufacturing process steps is provided. Description of operation as MW power amplifier and as power switching device is given. Theoretical breakdown voltage and ON-state resistance, power device theoretical limitations and premature breakdown mechanisms are discussed in details.

Chapter 3 gives overview on GaN-based HEMTs physical based device simulation as an engineering tool for design, analysis and evaluation of innovative concepts. Introduction to the physical-based models, structure definition and geometrical meshing is given. Nitride semiconductor material properties and their physical models are reviewed. Empirical parameters matching and adjustment of models parameters to match the experimental device measured results are discussed.

Chapter 4 presents systematic study of AlGaN/GaN/AlGaN DH-HEMTs as a possible solution for breakdown voltage enhancement. The physical-theory introduction to the DH-HEMTs is given along with simulation insight. Realization and fabrication of DH-HEMT devices on different substrates with parameters variation is demonstrated by multi-wafer experiments. Enhancement of the breakdown voltage by hundreds of volts with negligible influence on the ON-state resistance is shown. Comprehensive characterization in DC, robustness and reliability, and time and frequency domain is performed. Optimization of the DH-HEMT design parameters is discussed.

Chapter 5 demonstrates AlGaN/GaN/GaN:C back-barrier based HEMTs for state-of-the-art high breakdown voltage power switching devices. GaN carbon doping back-barrier concept is explained. Electrical DC characterization shows considerable reduction in the subthreshold leakage currents that result in breakdown voltage above 1000 V with very low ON-state resistance. Special attention is given to current-collapse phenomena in the manufactured devices.

Chapter 6 presents an innovative concept of Multiple Grating Field-Plates (MGFPs) integrated in DH-HEMTs. Physical insight to the mode of operation is given using physical based simulations. Electrical DC characterization discloses breakdown voltage enhancement of hundreds of volts. Minor tradeoff in current-collapse, time and frequency domain parameters is shown.

Dieses Werk ist copyrightgeschützt und darf in keiner Form vervielfältigt werden noch an Dritte weitergegeben werden.
Es gilt nur für den persönlichen Gebrauch.

Chapter 7 introduces GaN-based HEMTs with reverse blocking capability for Class-S switch mode amplifiers. The high voltage protection achieved by introducing recessed Schottky contact as a drain electrode. Such configuration provides protection of reverse bias over 110 V. Robust process integration is demonstrated. Devices are characterized in DC, large signal microwave power analysis, current collapse and switching test.

Chapter 8 introduces layout design and manufacturing technique examples for high voltage GaN-based HEMTs. Smart layout prevent immature breakdown due to lateral proximity of highly biased interconnects. Optimization of inter-device isolation designed for high voltage prevents substantial subthreshold leakage.

Chapter 9 concludes the results obtained in this work and summarizes results obtained. An outlook is given for future work towards optimization of GaN-based power switching electronic devices.

Dieses Werk ist copyrightgeschützt und darf in keiner Form vervielfältigt werden noch an Dritte weitergegeben werden.
Es gilt nur für den persönlichen Gebrauch.

Chapter 2

Fundamentals of GaN-based HEMTs Device and Technology

Fundamental background on GaN-based HEMTs material system, devices and technology are introduced in this chapter. First, the basic material properties and parameters of Gallium Nitride (GaN)-based semiconductors and their merits as a power electronics material are reviewed. GaN-based High Electron Mobility Transistors (HEMTs) physical principal of operation is described. Polarization effects in GaN-based semiconductor particularly for $Al_xGa_{1-x}N$/GaN heterostructures are introduced. Brief review of $Al_xGa_{1-x}N$/GaN HEMTs as microwave power amplifier and power switching transistor is given. Theoretical background on device breakdown and ON-state resistance in semiconductor unilateral device is introduced and the theoretical limits are calculated. Finally, a summary of the most common premature breakdown mechanisms in GaN-based HEMTs are reviewed.

Dieses Werk ist copyrightgeschützt und darf in keiner Form vervielfältigt werden noch an Dritte weitergegeben werden.
Es gilt nur für den persönlichen Gebrauch.

2.1. Introduction to GaN-Based Semiconductors and AlGaN/GaN HEMTs

Wide-bandgap semiconductor Gallium Nitride (GaN)-based material systems is standing in the center of attention of this work. Since its emergence in the early 1990s, GaN has attracted attention as highly promising material system for both optical and electronic applications. Over the last twenty years researchers from all over the world have made large efforts to transfer its potential into commercialization. GaN-based material systems are very interesting for electronic applications due to their wide-bandgap, excellent transport properties, high critical field and high thermal stability.

Fast development and performance demonstrations of GaN-based microwave and power devices in the last decade made it at present attractive alternative to Si-based power IGBTs and MOSFET high-end products. GaN-based transistors may bring about a revolution in power amplifier circuits for mobile phone base-stations, and power supply, motor drive and other circuits in fields including industrial equipment, white goods and automobiles. Compared to existing Si devices, they combine lower power losses with output up to ten times more, yielding circuits that are smaller and draw less power than ever. Though, it is far from perfection. Natural normally-on characteristics vs. normally-off requirements play a significant role for power switching.

GaN-based semiconductor devices offer five key characteristics: high dielectric strength, high operating temperature, high current density, high-speed switching and low ON-resistance, see Figure 2.1–1. These characteristics are due to the properties of GaN which include electrical breakdown characteristics ten times higher than that of Si, carrier mobility as good or better than that of Si, and a bandgap three times or more that of Si.

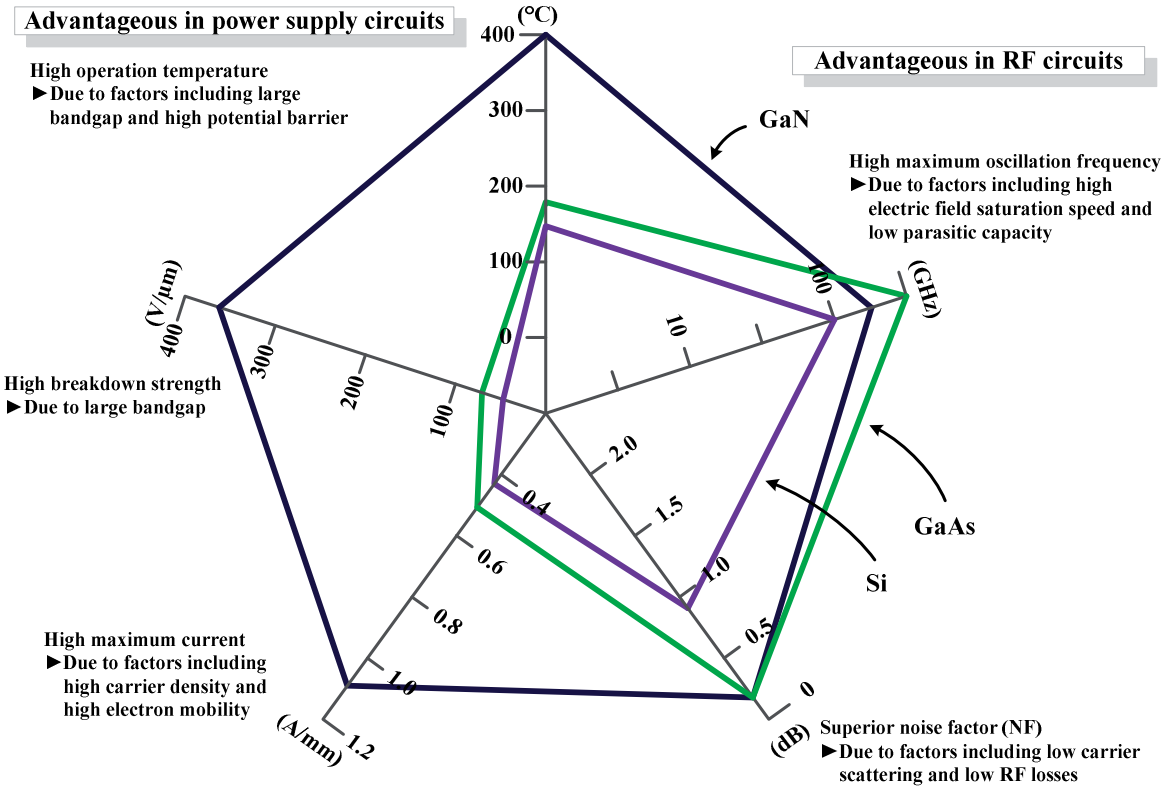

Figure 2.1–1 GaN material merits compared to Si and GaAs [19].

Dieses Werk ist copyrightgeschützt und darf in keiner Form vervielfältigt werden noch an Dritte weitergegeben werden.
Es gilt nur für den persönlichen Gebrauch.

Generally, to achieve high currents and high frequency operation in a semiconductor device, high charge carrier mobility (μ) and high saturation velocity (v_{sat}) are desirable. The high value for electron mobility of GaAs (8500 $cm^2 V^{-1} s^{-1}$) is the main reason that field-effect transistors (FETs) fabricated from this material have such excellent high-frequency performance (see Figure 2.1–1). A primary disadvantage of fabricating transistors from bulk GaN is the relatively low values for the electron mobility, which are ~900 $cm^2 V^{-1} s^{-1}$. However, these values are sufficient for transistors specifically designed for high-power operation. In general, wide-bandgap semiconductors have relatively low mobility but very high values for the saturation velocity, which is reached at high electric fields that can easily be supported (see sections 2.1.3 and 2.1.4 below). The mobility and saturation velocity of the 2DEG at the $Al_xGa_{1-x}N/GaN$ heterojunction is very suitable for high-power and high-frequency device applications. The room temperature mobility of the 2DEG, which is typically between 1200 $cm^2 V^{-1} s^{-1}$and 2000 $cm^2 V^{-1} s^{-1}$, is significantly better than that of bulk GaN. The 2DEG sheet charge density (n_s) of the $Al_xGa_{1-x}N/GaN$ structure is very high (experimental values up to 1×10^{13} cm^{-2}) due to piezoelectric and spontaneous polarization induced effects.

2.1.1. Material Structure and Polarization Wurtzite GaN-Based Semiconductors

GaN-based and other group III-N based semiconductors exist under different crystal structures, Wurtzite, Zinkblende and Rock-salt [20], [21]. At ambient conditions Al/In/Ga-N alloys present a thermodynamically metastable Wurtzite structure (WZ or 2H). The absolute majority of AlGaN/GaN HEMTs being grown on the Wurtzite phase, only this crystal structure will be farther considered. The Wurtzite structure has a hexagonal unit cell and consists of two intercepting Hexagonal Closed Packed (HCP) sub-lattice. Hence it is defined by two lattice parameters, a_0 and c_0, in ideal ratio $c_0/a_0 = \sqrt{8/3} \approx 1.633$, as shown in Figure 2.1–2. Each sub-lattice is constituted by one type of atoms which are shifted with respect to each other along the c axis by the amount $u_0 = 3/8$ in fractional coordinates. Because of the different metal cations, the bond lengths and the resultant c_0/a_0 ratios of the common nitride compounds AlN, GaN, and InN and their alloys are different. As the lattice non-ideality increases, c_0/a_0 ratio moves away from 1.633 of the ideal lattice [22].

Wurtzite GaN-based semiconductors and other group III-N based semiconductors; have a polar axis resulting from a lack of inversion symmetry in the <0001> direction. Owning to the difference in electronegativity (here given in Pauling's scale) between the Gallium (1.81) and/or Aluminum (1.61) and/or Indium (1.78), atoms and the Nitrogen (3.04) atom, the group III-N's are characterized with high ionicity of the metal-nitrogen covalent bond. Due to this electronic charge redistribution inherent to the crystal structure the group III-N semiconductors exhibit exceptionally strong polarization. This polarization refers to spontaneous polarization, P_{sp}, [22]. Because of their Wurtzite structure, GaN-based and group III-N based semiconductors can have different polarities, resulting from uneven charge distribution between neighboring atoms in the lattice. The polarity of the crystal is related to the direction of the group III-N dipole along the <0001> direction. Figure 2.1–2 shows the two possible polarities, in cation-face, i.e. Ga-face (a), structures the polarization field points away from the surface to the substrate, while in anion-face, i.e. N-face (b), structures the direction of the polarization field is inverted.

Dieses Werk ist copyrightgeschützt und darf in keiner Form vervielfältigt werden noch an Dritte weitergegeben werden.
Es gilt nur für den persönlichen Gebrauch.

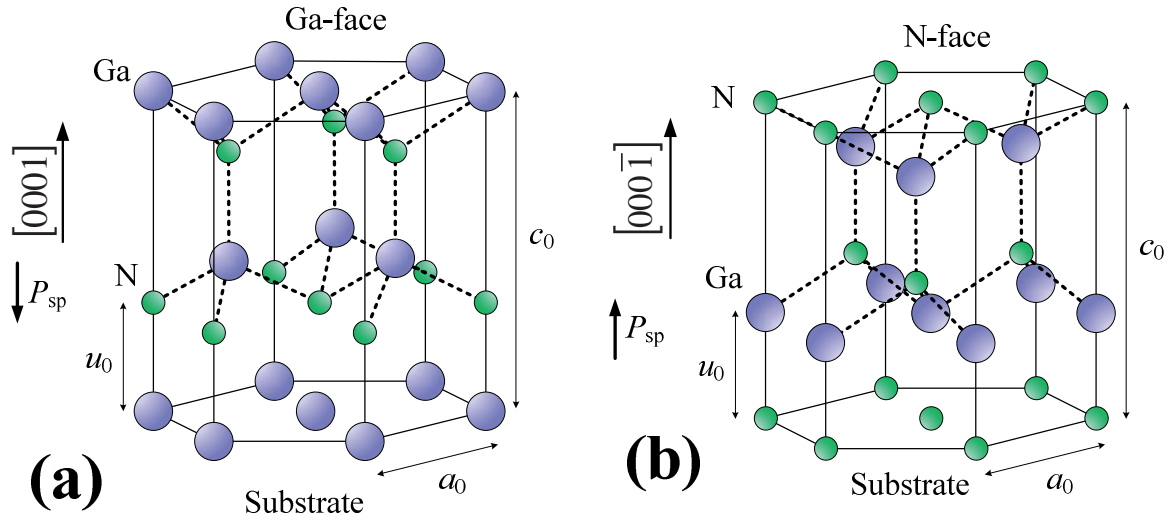

Figure 2.1–2 Illustration of (a) Gallium-face (b) Nitrogen-face ideal Wurtzite GaN lattice structure.

Due to this lack of inversion symmetry, when stress is applied along the <0001> direction to the group III-N semiconductors' lattice, the ideal lattice parameters c_0 and a_0 of the crystal structure will change to accommodate the stress. Therefore, the polarization strength will be changed. This additional polarization in strained group III-N crystals is called piezoelectric polarization, P_{pe} [22]. For example, if the nitride crystal is under biaxial compressive stress, the in-plane lattice constant a_0 will decrease and the vertical lattice constant c_0 will increase. Hence, the c_0/a_0 ratio will increase towards 1.633 of the ideal lattice and the total polarization strength of the crystal will decrease because the piezoelectric and spontaneous polarizations will act in the opposite directions. It is clear that if tensile stress is applied to the crystal, the total polarization will increase because the piezoelectric and spontaneous polarizations in that case act in the same direction. The piezoelectric polarization, P_{pe}, is simply expressed via the piezoelectric coefficients e_{33} and e_{13} as:

$$P_{pe} = e_{33}\varepsilon_3 + e_{13}(\varepsilon_1 + \varepsilon_2) \qquad 2\text{–}1$$

where a_0 and c_0 are the equilibrium values of the lattice parameters, $\varepsilon_3 = (c - c_0)/c_0$ is the strain along the c axis, and the in-plane strain $\varepsilon_1 = \varepsilon_2 = (a - a_0)/a_0$ is assumed to be isotropic. The different strains in the lattice are related as in:

$$\varepsilon_3 = -2 \cdot \frac{C_{13}}{C_{33}} \cdot \varepsilon_1 \qquad 2\text{–}2$$

where C_{13} and C_{33} are elastic constants. Eq. 2–1 and Eq. 2–2 can be combined to obtain the following equation:

$$P_{pe} = 2 \cdot \frac{a - a_0}{a_0} \cdot \left[e_{13} - e_{33} \frac{C_{13}}{C_{33}} \right] \qquad 2\text{–}3$$

Since in the wurtzite III-nitrides the piezoelectric coefficient e_{13} is always negative while e_{33}, C_{13}, and C_{33} are always positive, it turns out that $(e_{13} - e_{33} \cdot C_{13}/C_{33})$ will always be negative [20], [22]. As a consequence, the value of piezoelectric polarization (P_{pe}) in group III-N is always negative for layers under tensile stress ($a > a_0$) and positive for layers under compressive stress ($a < a_0$). As spontaneous polarization in group III-nitrides is always negative, it can be concluded that for layers under tensile stress, spontaneous and piezoelectric

Dieses Werk ist copyrightgeschützt und darf in keiner Form vervielfältigt werden noch an Dritte weitergegeben werden.
Es gilt nur für den persönlichen Gebrauch.

polarizations are parallel to each other (as shown in Figure 2.1–3(b)), and for layers under compressive stress the two polarizations are anti-parallel (as shown in Figure 2.1–3(a)).

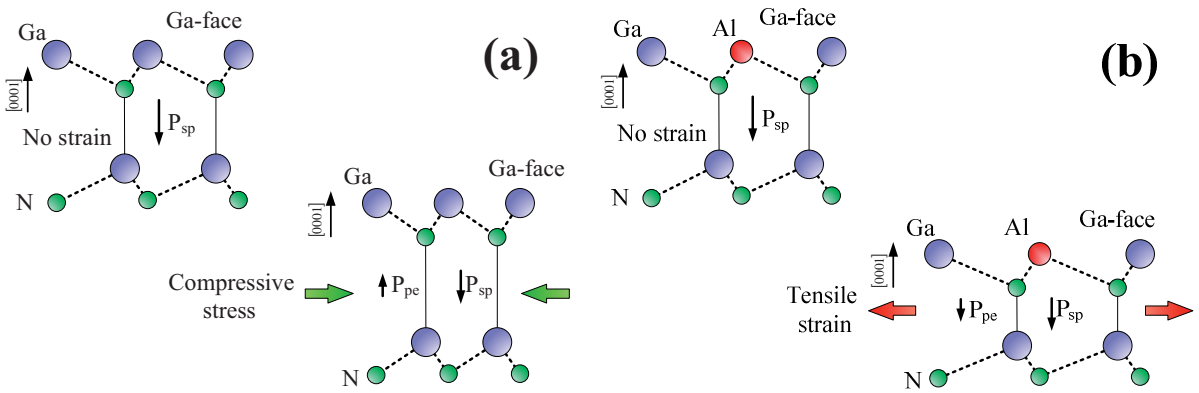

Figure 2.1–3 Illustration of (a) GaN Wurtzite Ga-face compressive stress. (b) AlGaN Wurtzite Ga-face tensile strain.

Polarization itself and gradients in polarization at interfaces and surfaces of AlGaN/GaN heterostructures induce fixed sheet charges, which in turn cause strong electric fields inside every heterostructure. In the nitrides the electric field can reach strength of 3×10^6 V/cm and therefore enhance electron or hole accumulation (depending on the polarity of the material) at AlGaN/GaN interfaces. This accumulation is known as polarization induced doping that is the source of the Two-Dimensional Electrons Gas (2DEG) that will be discussed in the following section.

2.1.2. $Al_xGa_{1-x}N$/GaN Heterostructures and 2DEG Formation

The most unique feature of the HEMT is channel formation from carriers (in our case electrons) accumulated along a heterojunction in a quantum well that are usually referred to as a Two-Dimensional Electrons Gas (2DEG) [23]. These electrons show enhanced mobility due to significantly reduced Coulomb scattering as they are separated from the top supply layer atoms from which they stem. In addition, mobility is further enhanced because of strongly reduced impurity scattering as the quantum well resides in the unintentionally doped, UID, material. Enhanced electron mobility is the key feature that differentiates HEMTs from ordinary FETs.

In early generation AlGaAs/GaAs-based HEMTs the origin of the carrier is a junction between a heavily doped high bandgap and a lightly doped low bandgap region. In GaN-HEMTs based structures, this carrier accumulation is mainly due to polarization charges developed along the heterojunction in the high bandgap AlGaN side. An $Al_xGa_{1-x}N$/GaN heterostructure is shown in Figure 2.1–4.

In Figure 2.1–4(a) the Fermi levels E_F of the two semiconductors do not coincide. At a real heterostructure in thermodynamic equilibrium, this will lead to a bending of the bands, until the structure will have just one common Fermi level (Figure 2.1–4(b)). The heterostructure results in the formation of a discontinuity in the conductance (E_C) and valence (E_V) band at the heterojunction. A triangular quantum well emerges, filled with electrons diffusing from semiconductor II and thus the strongly localized 2DEG develops. The term 2DEG refers to the condition in which electrons have quantized energy levels in one spatial direction but are free to move in the other two directions, parallel to the interface.

Dieses Werk ist copyrightgeschützt und darf in keiner Form vervielfältigt werden noch an Dritte weitergegeben werden.
Es gilt nur für den persönlichen Gebrauch.

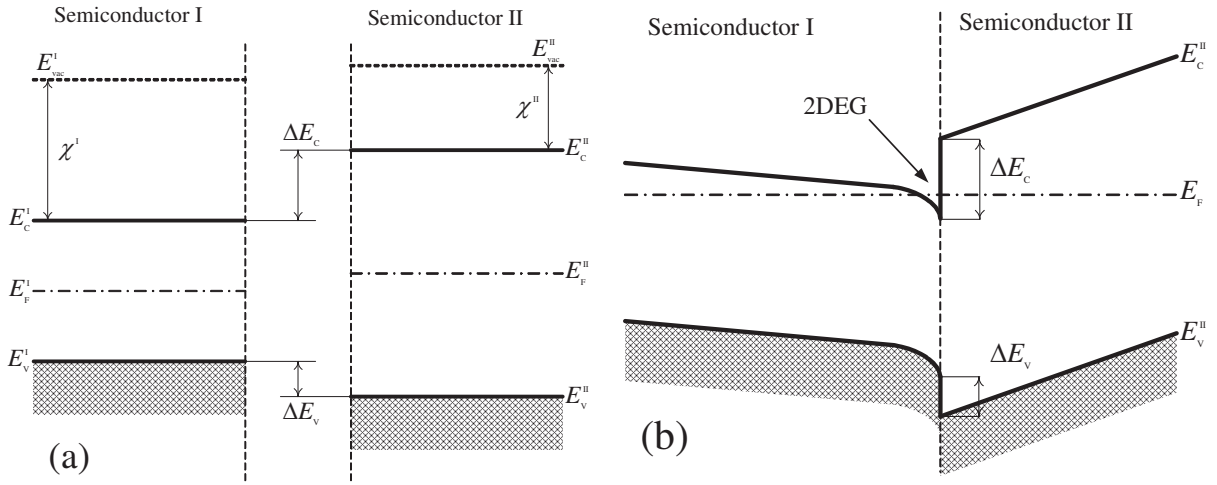

Figure 2.1–4 Band diagram of the heterostructure formed by polarized-piezoelectric narrow gap semiconductor I and polarized-piezoelectric wide gap semiconductor II, $a_I > a_{II}$ divided one from another (a) and together in thermo-dynamical equilibrium where semiconductor II is tensile strained (b).

It was shown that nitride epitaxial layers under stress exhibit both spontaneous and piezoelectric polarization fields. In general, if the polarization field ($\vec{P}$) changes in space, there will be a bound charge density (ρ) associated with it which is given by:

$$\rho = -\vec{\nabla} \cdot \vec{P} \qquad 2\text{–}4$$

For wurtzite III-nitrides polarization is always directed along the *c*-axis, perpendicular to the heterostructure interface. Hence, at the heterojunction, which is assumed to be planar and abrupt a bound sheet charge (σ) will be formed that is given by [24]:

$$\begin{aligned}\sigma &= \vec{P}_{(\text{top layer})} - \vec{P}_{(\text{bottom layer})} = \\ &= \left\{\vec{P}_{\text{sp}(\text{top layer})} + \vec{P}_{\text{pe}(\text{top layer})}\right\} - \left\{\vec{P}_{\text{sp}(\text{bottom layer})} + \vec{P}_{\text{pe}(\text{bottom layer})}\right\}\end{aligned} \qquad 2\text{–}5$$

This bound charge, which is induced by a change in polarization of the two layers, will attract compensating mobile charge at the interface. If the bound charge is positive it will cause a negative mobile sheet charge and vice versa. Baring this in mind we will focus on the calculation of bound charge and the corresponding 2DEG density in a Ga-face undoped AlGaN/GaN heterojunction as shown in Figure 2.1–5.

At the $Al_xGa_{1-x}N$/GaN interface, the difference in polarization between both materials leads to a polarization sheet charge:

$$\sigma = \vec{P}_{(\text{AlGaN})} - \vec{P}_{(\text{GaN})} \qquad 2\text{–}6$$

If this sheet charge density is positive, free electrons compensate this charge and form a two dimensional electron gas, 2DEG, assuming that the band structures of the materials at the interface allow this to happen. To calculate the amount of polarization induced sheet charge density at the interface between $Al_xGa_{1-x}N$ and GaN, material parameters for $Al_xGa_{1-x}N$ alloys can be calculated from the known Al mole fraction values of $0 \geq x \geq 1$ [25], [26]. The polarization induced sheet charge density is expressed as:

$$\sigma = \vec{P}_{\text{sp}(Al_xGa_{1-x}N)} + \vec{P}_{\text{pe}(Al_xGa_{1-x}N)} - \vec{P}_{\text{sp}(\text{GaN})} - \vec{P}_{\text{pe}(\text{GaN})} \qquad 2\text{–}7$$

The piezoelectric polarization for GaN $\vec{P}_{\text{pe}(\text{GaN})}$ is assumed to be zero since bulk GaN buffer layers are assumed none-strained and thus strain-free. Since $Al_xGa_{1-x}N$ grown on Ga-face GaN is always under tensile strain, both piezoelectric and spontaneous polarizations have the same sign and add up.

Dieses Werk ist copyrightgeschützt und darf in keiner Form vervielfältigt werden noch an Dritte weitergegeben werden.
Es gilt nur für den persönlichen Gebrauch.

The high positive polarization induced sheet charge density, formed at $Al_xGa_{1-x}N$/GaN interface for Ga-face layers, can be compensated by free electrons to form a two-dimensional electron gas (2DEG). It is not clear where the electrons come from: they can be attracted from the bulk GaN buffer layer or from donor-like surface states [27], or from carrier injection from the metal contacts [24]. The maximum sheet carrier concentration can be expressed as [25], [28]:

$$n_s(x)=\frac{\sigma}{q}-\frac{\varepsilon_0 E_F}{q^2}\left(\frac{\varepsilon_r(x)}{d(x)}+\frac{\varepsilon_{r(GaN)}}{d_{(GaN)}}\right)-\frac{\varepsilon_0\varepsilon_r(x)}{q^2 d(x)}[q\phi_b(x)+\Delta(x)-\Delta E_C(x)] \qquad 2\text{–}8$$

where $d(x)$ the thickness of the $Al_xGa_{1-x}N$ layer, E_F the position of the Fermi level with respect to the GaN conduction band at the GaN-substrate interface, $q\phi_b$ the Schottky barrier height of the gate contact on top of the $Al_xGa_{1-x}N$ layer, $\Delta(x)$ the position of the conduction band below the Fermi-level at the interface, and $\Delta E_C(x)$ the conduction band offset at the interface. This equation cannot be solved analytically. The middle term containing E_F is negligible if GaN buffers thicker than 1 µm are grown, and the expression reduces to that given in [24]. A schematic indication of the $Al_xGa_{1-x}N$ /GaN conduction band diagram is given in Figure 2.1–5.

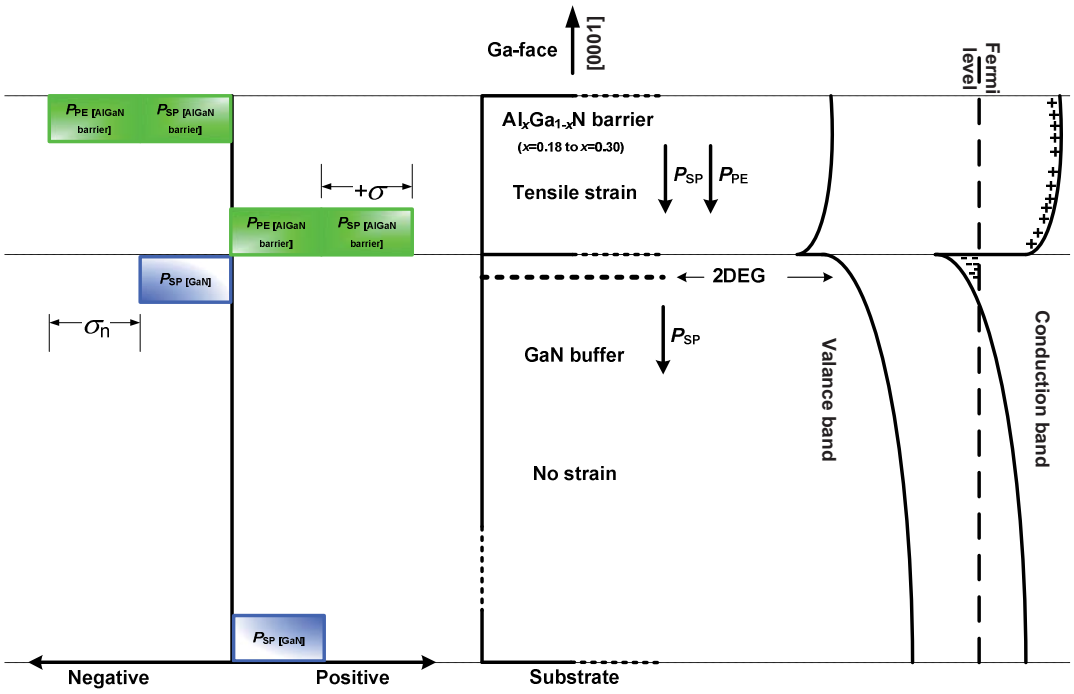

Figure 2.1–5 Polarization scheme and conduction band diagram of Ga-face $Al_xGa_{1-x}N$ /GaN-based HEMTs.

2.1.3. Carrier Mobility in $Al_xGa_{1-x}N$/GaN heterostructures' 2DEG

In power devices the resistance of the drift region can be drastically reduced by replacing narrow band gap semiconductor like silicon with wide band gap semiconductors like GaN-based semiconductors. The resistivity (ρ) of any semiconductor region is given by:

$$\rho=\frac{1}{q\mu N_n} \qquad 2\text{–}9$$

where μ by the mobility, which is a function of the carrier (electrons) concentration (N_n).

Dieses Werk ist copyrightgeschützt und darf in keiner Form vervielfältigt werden noch an Dritte weitergegeben werden.
Es gilt nur für den persönlichen Gebrauch.

In any semiconductors, carriers are accelerated by the presence of an electric field and achieve an average velocity determined by the carrier scattering processes. As the free carriers are transported along the direction of the electric field, their velocity increases until they experience scattering. In the bulk semiconductor, the scattering can occur either by interaction with the lattice or at ionized donor and acceptor atoms. Consequently, the mobility is dependent upon the lattice temperature and the ionized impurity concentration. The low field mobility (μ) is defined as the proportionality constant relating the average carrier velocity (v_D) to the electric field (E):

$$v_D = \mu E \qquad 2\text{–}10$$

This expression is valid at low electric fields. However, in power devices the high electric field presents then the velocity is no longer found to increase in proportion to the electric field. In fact, the velocity approaches a constant value known as the saturated drift velocity. (See section 2.1.4 below)

As the carriers travel through a semiconductor, they undergo a variety of interactions with the host material. The electron mobility is the most popular and most important transport parameter used to characterize the microscopic quality of the semiconductor layers. Mobility is considered to be the figure of merit for materials used for electronic devices.

In addition to the high carrier concentration in the 2DEG created by the polarization induced doping at the AlGaN/GaN interface; carriers in the 2DEG have unique high mobility properties. GaN-based semiconductors' large bandgap, large dielectric breakdown field, good electron transport properties (an electron mobility possibly in excess of 2000 $cm^2\ V^{-1}\ s^{-1}$ and a predicted peak velocity approaching 3×10^7 cm s^{-1} at room temperature), and good thermal conductivity are merits for high-power/temperature electronic devices.

In AlGaN/GaN-based HEMTs, the carriers that form the 2DEG channel in the smaller bandgap material, UID GaN, are donated by the larger bandgap material, AlGaN. Because the mobile carriers and their parent donors are spatially separated, short-range ion scattering is nearly eliminated, which leads to mobilities that are characteristic of nearly pure semiconductors.

Electron mobility is a key parameter in the operation of GaN-based HEMT as it affects the access resistances as well as the rate with which the carrier velocity increases with electric field. Consequently, the low-field mobility in GaN is depending on various scattering events. The electron mobility is limited by the interaction of electrons with phonons and, in particular, with optical phonons. This holds for bulk mobility as well as that in AlGaN/GaN HEMTs' 2DEG.

Khan *et al*. showed in their early work, illustrated in Figure 2.1–6, mobility for the single GaN layer increases from 450 $cm^2\ V^{-1}\ s^{-1}$ at room temperature to 1200 $cm^2\ V^{-1}\ s^{-1}$ at 150 K. It then decreases for lower temperatures due to ionized impurity scattering. On the other hand, the electron mobilities of the heterojunction increases from 1500 $cm^2\ V^{-1}\ s^{-1}$ at room temperature to a value of 5000 $cm^2\ V^{-1}\ s^{-1}$ at 150 K and remains essentially constant for temperatures down to 80 K. This enhanced electron mobility is associated to the presence of 2DEG at the hetero-interfaces. The 2DEG mobility enhancement is caused by a much higher volume electron concentration (compared to the bulk *n*-GaN), which results in a larger Fermi energy and a more effective screening [29], [30].

Dieses Werk ist copyrightgeschützt und darf in keiner Form vervielfältigt werden noch an Dritte weitergegeben werden.
Es gilt nur für den persönlichen Gebrauch.

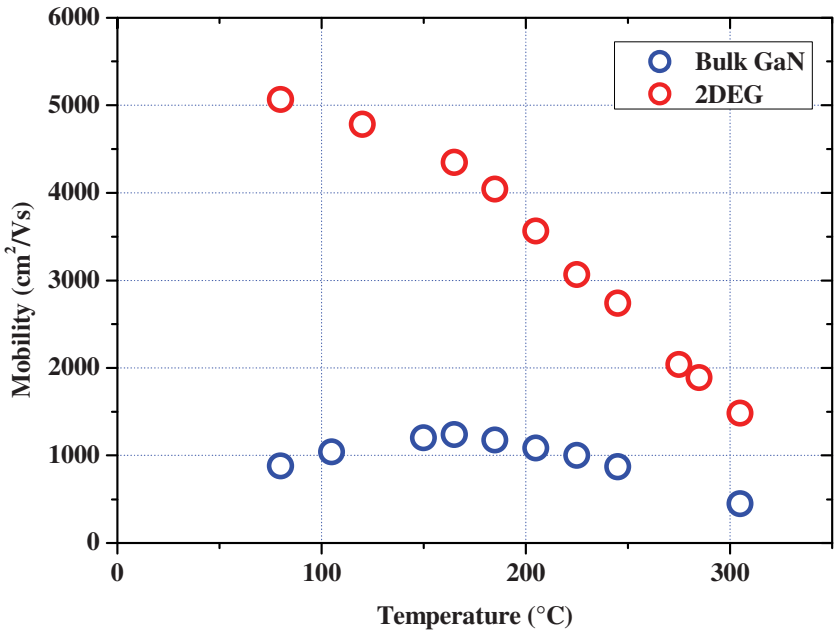

Figure 2.1–6 Experimental electron Hall mobility in GaN vs. temperature for $Al_{0.1}Ga_{0.9}N$/GaN two dimensional electron gas (2DEG) and bulk *n*-GaN $n = 1 \times 10^{17}$ cm^{-3}. (Results are taken from [29])

The 'traditional' scattering mechanisms in 2DEG and their effects on the carrier mobility have been studied for AlGaAs/GaAs and Si-MOSFET systems. They are important in AlGaN/GaN 2DEG transport as well. Electrons moving in the 2DEG experience interface-roughness scattering due to the non-abrupt interface between AlGaN and GaN. The 2DEG wave-function is mostly confined in GaN, but there is a finite part that penetrates the AlGaN barrier, leading to alloy-disorder scattering. Interface-roughness scattering and alloy scattering are short-range scattering sources [31]. Charged impurities are always present in the semiconductors samples, and constitute a form of long-range Coulombic scattering source. The lattice vibrates at finite temperatures and phonons form a potent scattering mechanism at high temperatures. An important form of Coulombic scattering in AlGaN/GaN 2DEGs is dislocation scattering, owing to the large density of dislocations in the material. The cores of threading edge dislocations have dangling bonds that introduce states in the gap of the semiconductor, causing a dislocation to become a line of charge. Such charged dislocations scatter conduction electrons. Dislocations also scatter from strain-fields that develop around them.

Due to the very high electric fields that result from the large polarization (~ 1 MV/cm), electrons in the 2DEG are electro-statically pushed close to the AlGaN/GaN interface, and the centroid of the wave function is brought closer to the hetero-interface. This directly leads to an increased sensitivity to alloy disorder and interface roughness scattering, which turn out to be the dominant scattering processes at low temperatures, and even at room temperature for very high density 2DEGs. In addition the microscopic disorder in an alloy layer, the dipole moment in each unit cell is no more periodic with the crystal lattice; therefore it leads to 'dipole-scattering'. This interesting novel scattering mechanism has no analogue in traditional non-polar and weakly-polar semiconductors.

For the design of GaN-based HEMTs structures specially for high power devices with high conductivity the following should be taken into consideration [32]; Mobility of low-density AlGaN/GaN 2DEGs ($n_{2DEG} \leq 10^{12}$ cm^{-2}) is limited by scattering from charged defects such as dislocations, dipoles, residual impurities. Mobility of high-density AlGaN/GaN 2DEGs is insensitive to scattering by various charged impurities. Alloy disorder scattering limits the mobility for AlGaN/GaN 2DEGs at low temperatures. At extremely high carrier densities, alloy scattering is as severe as scattering from phonons, even at room temperature.

Dieses Werk ist copyrightgeschützt und darf in keiner Form vervielfältigt werden noch an Dritte weitergegeben werden.
Es gilt nur für den persönlichen Gebrauch.